



EXPERIMENTAL INVESTIGATION OF PRECAST CONCRETE BEAM TO COLUMN CONNECTIONS SUBJECTED TO REVERSED CYCLIC LOADS

H. Shariatmadar¹, E. Zamani Beydokhti²

¹Department of Civil Engineering, Ferdowsi University of Mashhad, Mashhad, Iran,
(Shariatmadar@um.ac.ir)

²Ph.D student, Department of Civil Engineering, Ferdowsi University of Mashhad, Mashhad, Iran,
(Ebrahim.zamany@gmail.com)

ABSTRACT

Two types of precast and one type of monolithic full scale beam-column connections are tested under reversed cyclic loads. Both of the precast concrete connections tested were cast in place, but with different connection details, namely straight spliced (PC1) and U-shaped (PC2). The straight spliced and U-shaped connections were located in the beam and column of the precast concrete subassemblies. Hysteresis response, strength, stiffness, damping and energy dissipation of monolithic and precast connections were studied and then compared together. Monolithic specimen (MO) indicated a good behavior in terms of integrated seismic parameters. The experimental results shows that Specimen PC1 in which the top and bottom reinforcement are continued by lap splicing treated a good behavior very similar and closed to those of control monolithic specimen and performed very good based on seismic demand. The behavior of Specimen PC2 that U-shaped rebars were used in its connection was not satisfactory in comparison with other specimens. Some shear deteriorations observed in both PC1 and PC2 connections. As conclusion, connections PC1 and PC2 are suggested in precast moment resisting frames with moderate ductility located in high seismic zones. However, some essential practice-oriented modifications are required.

Keywords: Precast Concrete Connections, Moment Resisting Frames, Reversed Cyclic Loads, Energy Dissipation, Ductility Ratio

1. INTRODUCTION

Precasting has several advantages that can emulate conventional cast-in-place construction and satisfy us to give more attentions to researching for more suitable connection details. High quality control, construction efficiency and consequently saving in time and expenses are some of precasting advantages. Nevertheless we have some problems that are resulted due to assembling the precast members such as beams and columns. The joints created with time differences between connection and its surrounding concrete are the most weakness links in precasting and very exposed to plastic hinge generation. Since there is no building code specified for precast structures, all designs are done with cast in place concrete design codes in Iran, beam-column connections must designed in another method. For this reason we have no way to behavior evaluation of these structural elements except experimental studies. As a result,

a research program on the performance of ductile beam-column precast connections was evaluated in Ferdowsi University of Mashhad [1]. Two precast connections with straight spliced and U-shaped in column region were tested and compared with its monolithic counterpart. Performance comparisons are made according to strength predictions, stiffness degradation, damping, ductility and energy dissipation of the connections. All test specimens in this research program are detailed according to the governing building codes or the available literature.

2. LITERATURE SURVEY

Connection detailing and its location between precast members is one of numerous either experimental or analytical investigation issues for researchers. Ertas et.al [2] tested four types of cast in place precast (CIP) beam-column connections tested with reversed cyclic loading in inelastic range. Specimens were subjected to 3.5% story drift angle in ultimate loading. The hysteresis behavior of cast in place column, cast in place beam, and modified bolted specimens were similar to those of monolithic specimen. Pinching effect and excessive bond deterioration were not observed in the CIP connections due to the use of steel fiber concrete. A research consisted of precast concrete beams placed between columns and a CIP concrete joint core that was constructed between the beam joining ends performed by Restrepo [3]. The test results showed that the connection detail can be successfully designed and constructed to emulate cast-in-place construction. Alcocer et.al [4] tested two full-scale precast beam-to-column connections under uni-or bi-directional cyclic loading. Conventional mild steel reinforcing bars or prestressing strands, rather than welding or special bolts, were used in specimens.

3. TEST SPECIMENS AND CONNECTION DETAILS

All full scaled specimens are selected from a five story peripheral frame with two beams in one plane that connected to column faces. Two cross shaped precast specimens (PC1& PC2) and one monolithic counterpart (MO) were designed and manufactured according to strength and stiffness demand and calculated with Iran's concrete building code (ABA). Free span length and cross section of beams are 200cm and 40x40cm, respectively. Total length of specimen columns was 320cm that beams were connected to its faces in mid height. All reinforcing bars were AIII type, precast concrete designed for 280Mpa compressive strength. The concrete mixture of cast in place connections in laboratory was similar to the precast members and monolithic specimen.

3.1. MONOLITHIC SPECIMEN

Monolithic specimen (MO) developed for comparison with precast specimens results designed according to Iran's cast in place (CIP) concrete recommendations (ABA). As shown in Figure 1 the column longitudinal reinforcement was 8 ϕ 18 for all specimens.

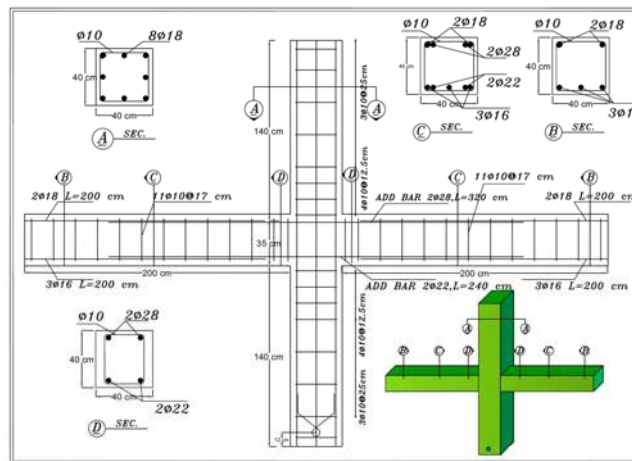


Figure 1. Dimensions and reinforcement details of Monolithic Specimen

Spacing of the closed stirrups $\phi 10$ was approximately 125 mm at the 70cm top and bottom of beam-column joint core and 250 mm at the remaining length of column. The top and bottom longitudinal bars of beams were $2\phi 18$ and $3\phi 16$, respectively, where some ADD-bars were added to these rebars. ADD-bars are placed in connection region were $2\phi 28$ at the top and $2\phi 22$ at the bottom. These bars have 320 cm and 240 cm length in top and bottom, respectively. Top ADD-bar's area is increased for realization due to gravity load effect.

3.2. STRAIGHT SPLICED SPECIMEN

Figure 2 shows the details for straight spliced specimen (PC1). The design concept of Specimen PC1 was for most similarity with Specimen MO. Column reinforcing was the same as MO ($8\phi 18$). There was a gap at midheight of the precast concrete column. The height of the gap was 35 cm and was a little less than the depth of beam. There was a box shaped free space in PC1 beams at the vicinity of column face for placing the ADD-bars. The number and diameter of main longitudinal and ADD-bars of beams were the same as MO's. After placing the beams at axe of the column's gap and entering the ADD-bars in free gap of column, column's and beam's free spaces with top 10 cm of precast beams were filled with cast in place concrete with 26 Mpa compressive strength.

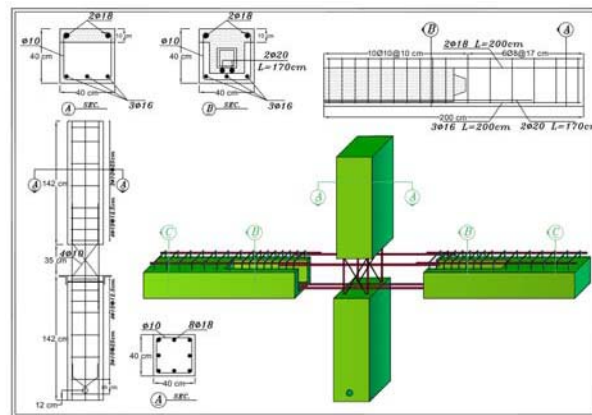


Figure 2. Dimensions and reinforcement details of Specimen PC1

3.3. U-SHAPED REBAR SPECIMEN

The details of U-shaped specimen (PC2) are presented in Figure 3. The aim of using U-shaped rebars is to minimize the splicing length need of field working area and to develop the full strength in a bar in vicinity of column faces. The column configuration of Specimen PC2 was exactly equal to that for Specimen PC1.

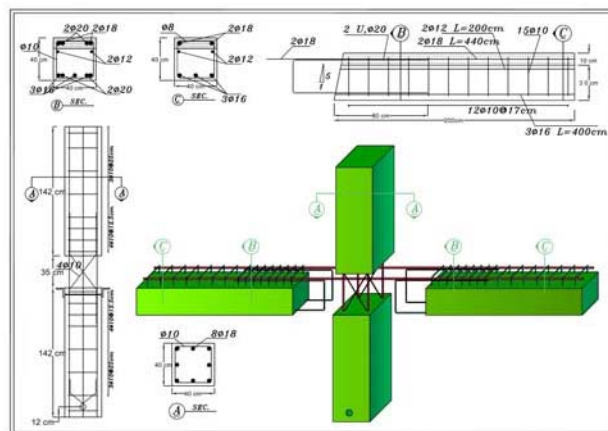


Figure 3. Dimensions and reinforcement details of Specimen PC2

Two U-shaped rebars in beams were entered to free gap of column mid-height from each side. Four U-shaped rebars of PC2 were $\text{f}20$. Top main rebars of PC2's beam were $2\text{f}18$ with 440 cm length that were fixed after assembling the beams and column together. Bottom main rebars of beams were $3\text{f}16$ with 200 cm length. The properties of concrete and reinforcement place in connection region were equal for the both specimens.

4. TESTING PROCEDURE

The circumstances of carrying out the test setup were in a new manner. Figure 4 shows the test set-up and measuring instruments. The test specimens were initially situated in horizontal plane on some rollers to move freely and then boundary conditions were installed. For applying points of contra flexure in frame members due to lateral loads, the supports of test set-up in column bottom and end of beams were pinned and roller, respectively. Axial force was applied to column bottom with a hydraulic jack. Lateral loading was applied gradually to column top, mostly with displacement control, until achieving to desired drift angle.

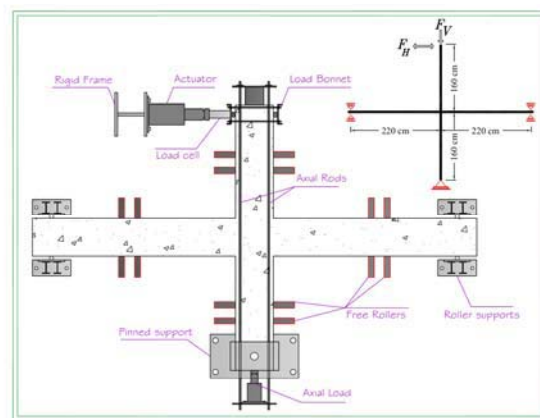


Figure 4. Test setup and instrumentations

An Ultra Sonic sensor was adjusted on a fixed frame closed to column top for measuring the lateral displacement. Bottom movement of the column in pinned support was fixed. Lateral load applied with a 20 ton hydraulic actuator to column top. As shown in Figure 4 a 50 ton load cell was located between actuator and loading bonnet. This bonnet was prepared to apply reversed cyclic lateral loading. Figure 5 shows lateral loading history for the test. Load laterally applied in primary cycles was load controlled and then was displacement controlled until maximum drift angle. Loading in stage1 was applied at observation of fine cracks. In the next stages, loads were applied at 1, 1.5, 2, 2.5 and 3% drift angle. Three cycles loading was applied in each drift level. At the end of cycle 18th, test of specimens were continued with repeating loading due to lack of actuator stroke. Crack widths were monitored at the end of each loading stages. Finally, test was terminated at 6% drift level.

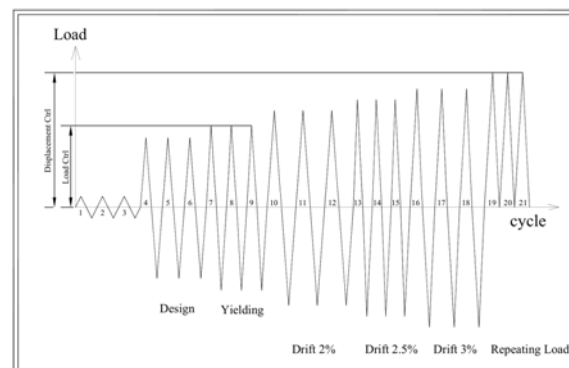


Figure 5. Typical loading history

5. TEST RESULTS

5.1. MONOLITHIC SPECIMEN (MO)

Load versus drift hysteresis response of Specimen MO is presented in Figure 6-a. The behaviour of the specimen in the first loading stage was nearly elastic and residual displacement was less than 0.5 cm. The first flexural cracks were occurred at 3.84 ton and 0.14% drift angle. After three cycles in this step, load was increased to design value of 5.12 ton according to ABA. Then loading was continued to yielding of longitudinal bars at the end of this load stage. In further loading stages, load was applied in displacement control regime in 2, 2.5 and 3% drift angle. Maximum crack width in 11 ton was 3mm and it increased to 5mm in 13.58 ton. Diagonal cracks were revealed in the beam-column connection region at cycle 10 (13 ton load). When drift angle reached to 3% - about 2 times of minimum required code value - the repeating loads was applied to specimen. Result showed that capacity didn't decrease significantly during reversed and repeating load cycles. Load capacities in forward and backward reversed cycles were measured to be 13.58 ton and 11.85 ton, respectively. Moment capacity was about 14.8ton.m which is near to calculated ultimate value (15.5 ton.m). Cracks took place mostly in the beam bottom due to using $\text{f}22$ instead of $\text{f}28$ used at beam top. A photo of crack pattern at 4% drift is shown in Figure 6-b.

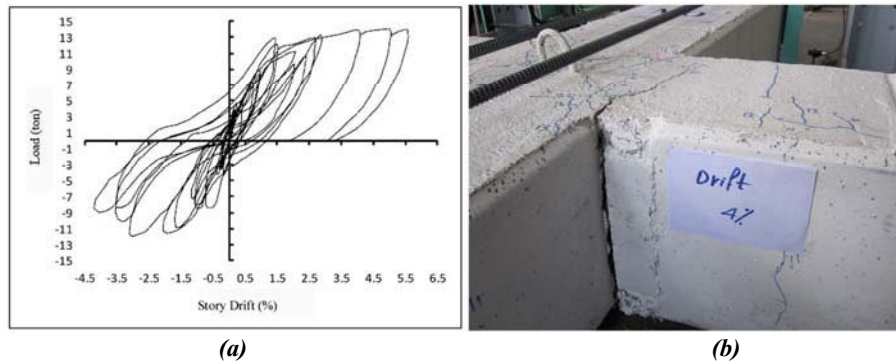


Figure 6. (a) Lateral load versus story drift for monolithic specimen
(b) Damage in monolithic specimen at 4% drift angle

5.2. STRAIGHT SPLICED SPECIMEN (PC1)

Load versus drift angle hysteresis curve for Specimen PC1 is shown in Figure 7-a. Overall behaviour of Specimen PC1 is very similar to Specimen MO, however diagonal and flexural cracks are more and wider for PC1. Initial obvious cracks were appeared in load of 4 ton. Cracks observed align the negative rebars on top of beam at second compressive loading. Positive and negative cracks reached together in 6.5 ton and their widths were 0.5mm. Cracks spread on middle of beams at fifth cycle.

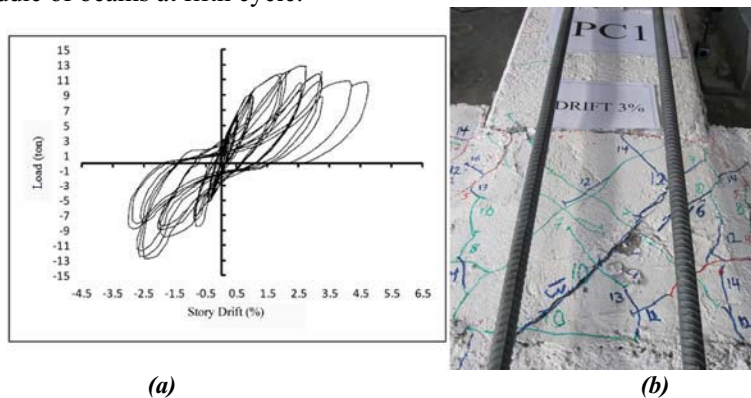


Figure 7. (a) Lateral load versus story drift for PC1 specimen
(b) Damage in PC1 specimen at 3% drift angle

Yielding was occurred at cycle 7 in 0.71% drift and 9.06 ton. Crack widths were opened more than 0.5mm and they reached from 0.7mm to 1.25mm due to yielding. After 3% drift in stage3, load capacity of the specimen was decreased severely from 13.5 ton to 11 ton. Loading was stopped at 6% drift angle and residual displacement reached to 11cm. Crack concentration was in connection core, and bottom of the beam was absolutely opened as can be seen in Figure 7-b. Load and moment capacities were approximately equal to 13ton and the 14.3ton.m, respectively. Hysteresis loops are slightly S-shaped where pinching is observed.

5.3. U-SHAPED REBAR SPECIMEN (PC2)

Hysteresis curve for Specimen PC2 is shown in Figure 8-a. Since rebar area in PC2 was less than MO and PC1 ($\rho=1.26\%$), it was expected that moment capacity in PC2 would be less than the others. Initial cracks were observed in 4.92 ton. Design load was applied in three cycles with 7.15 ton as calculated before. Diagonal crack created in joint core but the specimen was in elastic range yet. At load level of 7.45 ton, yielding of bar and diagonal shear cracks in beam were developed. The loading on specimen changed to displacement control after this level.

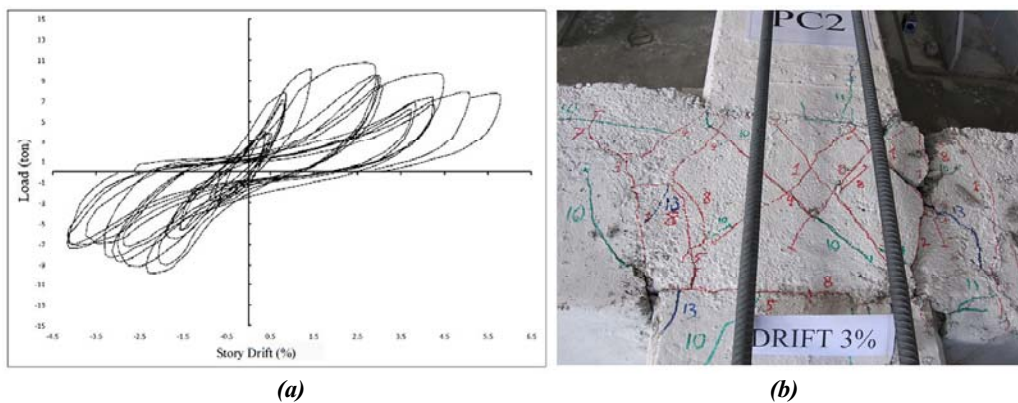


Figure 8. (a) Lateral load versus story drift hysteresis response for Specimen PC2
(b) PC2 Damage in Specimen PC2 at 3% drift angle

Pinching was occurred after 2% drift angle and loading was continued to 8.4 ton. Load carrying capacity was reduced to 6 ton in 2.5% drift level. In the first cycle in 3% drift angle, connection strength increased to 8.78 ton but after that, crack widening in remaining cycles in 3% drift eventually led to decreasing load capacity to 6.5 ton again and cover concrete in joint core was spalled and pulled off. The specimen capacity after 3% drift level could not be increased farther than 6.5 ton due to softening. Test was terminated in 4% drift angle in repeating load stage because of specimen failure. A closed-up photo of the damaged specimen and crack patterns at the 3% drift is presented in Figure 8-b.

6. EVALUATION OF TEST RESULTS

Seismic behaviour of the specimens MO, PC1 and PC2 were compared together with respect to dynamic parameters such as: stiffness degradation, energy dissipation, damping ratios and ductility factors. All of these parameters are non-dimensional values to eliminate different connection details and strengths.

6.1. STIFFNESS DEGRADATION

The slope of the curves can provide a relative measure for comparison of the secant stiffness of the specimens. Variation in specimen stiffness at the last cycle of each successive story drift level during the test under reversed cyclic loads is shown in Figure 9. It is normalized to 1 by dividing all stiffnesses in each cycle by initial stiffness at first cycle. Stiffness of PC1 was higher than the other specimens. Specimen PC2 shows a poor variation and its stiffness is decreased severely after first cycle. Initial stiffness of MO was very high and its damage in each

cycle was less than PC1 and PC2. The stiffness of specimens are approximately the same after 2% drift angle and they are decreased to zero in termination cycles due to pinching effect.

6.2. ENERGY DISSIPATION

Energy dissipation capacity of a connection is a function of the area under the load–deflection curve and it indicates how effectively a connection withstands earthquake loadings. The typical way of comparing the energy dissipation is to plot the cumulative dissipated energy against the number of cycles applied [6]. As it is shown in Figure 10 energy dissipation of MO is in ideal state Specimens PC1 and PC2 had an ascending trend but energy dissipation capacity of PC2 was higher than that for PC1.

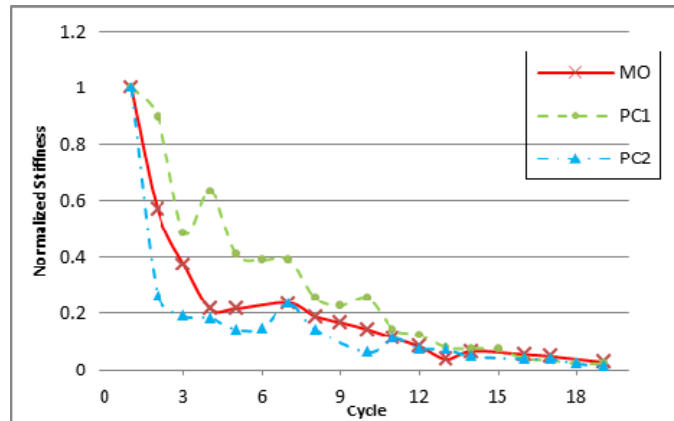


Figure 9. Stiffness degradation of specimens

These results might be depended on connection details and specimen's strength because energy is not a non-dimensional parameter.

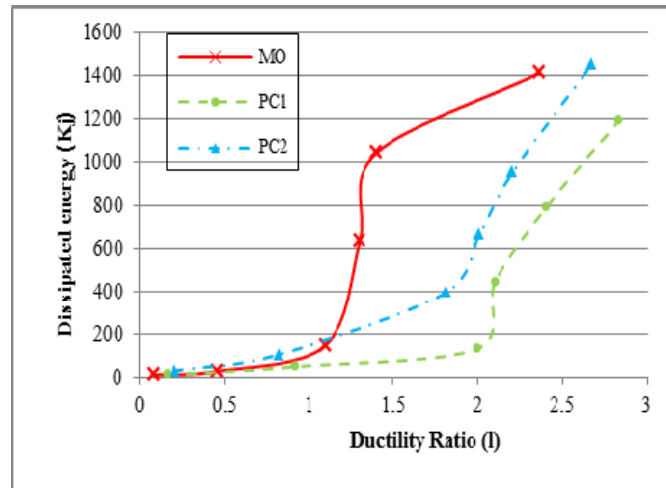


Figure 10. Dissipated energy versus ductility ratio for specimens

6.3. DAMPING RATIO

Damping ratio is a non-dimensional parameter to compare energy dissipation capacity in specimens contrary to previous parameter. To discuss the energy dissipation characteristics of the test specimens, the equivalent viscous damping ratio (ζ_{eq}) was plotted against the number of cycles. Viscose damping is defined by a coefficient of hysteretic energy (A_p) and elastic peak to peak strain energy (A_e) according to Figure 11 and Equation 1.

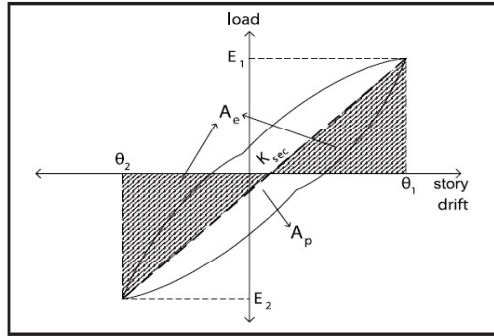


Figure 11. Representation of equivalent damping ratio [2]

$$\zeta_{eq} = \frac{1}{2\pi} \frac{A_p}{A_e} \quad (1)$$

Viscos damping has an unidentified regime during different drift levels. It starts from a value about 10% to 15%, maximizes in a middle cycle and ended with a lower value according to Figure 12.

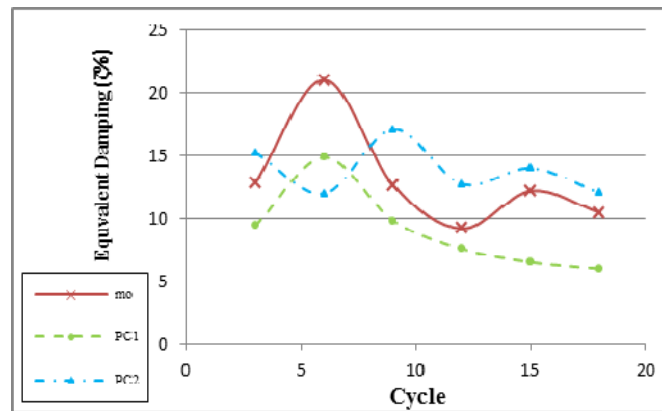


Figure 12. Equivalent damping ratio versus number of cycles for specimens

7. CONCLUSIONS

The Reversed cyclic loading experiments were performed on two types of precast concrete beam to column connection sub-frame systems and one monolithic counterpart. From this research, the following conclusions can be drawn:

- Behaviour of monolithic specimen was satisfactory in terms of strength and ductility and behavior of PC1 was very close to that. Pinching is occurred in precast specimens and it was more obvious in PC2 in higher drift levels.
- Specimen MO has no strength degradation until drift 4% whereas in PC1 it was 11% and 35% in PC1 and PC2, respectively.
- Stiffness degradation in PC1 was less than MO and PC2 until 2% drift angle. This parameter became similar in all of specimens up to 2% drift.
- Monolithic specimen had a good energy dissipation characteristic. Behaviour of PC2 was better than PC1 in terms of damping and energy dissipation but it damaged more severe and cracks was wider than PC1.
- All specimens had satisfactory seismic behaviour even until two times of almost all of building code requirements and they are applicable in moderate to high seismic zones.

5. REFERENCES

1. Zamani. B, E. (2010). "Building experimental investigation of precast concrete beam to

- column connections subjected to reversed cyclic loads", M. S. thesis, Ferdowsi University of Mashhad (in Farsi).
2. **Ertas, O., Ozden, S. and Ozturan. T.** (2006). "Ductile connection in precast concrete moment resisting frames ", PCI JOURNAL.
 3. **Restrepo, J. I., Park. R., and Buchanan. A. H.** (1995). "Tests on Connections of Earthquake Resisting Precast Reinforced Concrete Perimeter Frames of Buildings", PCI JOURNAL.
 4. **Alcocer, S. and others** (2002). "Seismic test of beam-to-column connections in a precast concrete frame", PCI JOURNAL.
 5. **Khoo. J. H., Li. B. and Yip. K. W.** (2006). "Tests on Precast Concrete Frames with Connections Constructed Away from Column Faces", ACI STRUCTURAL JOURNAL, Vol 103, NO. 1.
 6. **Korkmaz. H. H., Tankut. T.** (2005). "Performance of a precast concrete beam-to-beam connection subject to reversed cyclic loading" , Journal of Engineering Structures.